Numerical Simulation of Fast Atmospheric Electric Discharge in the Tip-to-Plane Configuration

V. Y. Kozhevnikov[1,2], A. V. Kozyrev[1,2], A. O. Kokovin[1,2] and V. S. Igumnov[3]
[1]Institute of High Current Electronics, 2/3 Akademichesky ave., 634055 Tomsk, Russia
[2]Tomsk State University, 36 Lenina ave., 634050 Tomsk, Russia
[3]National Research Tomsk Polytechnic University, Tomsk 634050, Russian Federation

Abstract. This paper deals with the results of numerical simulation of the fast atmospheric pressure discharge in strongly non-uniform configuration of a tip-to-plane diode filled with nitrogen and oxygen mixture. The simulation is based on the advanced hydrodynamic discharge plasma accounting also gas photoionization. It was shown that in the absence of photoionization discharge develops unstable and photoionization suppresses this instability. Theoretical results fits the existing experimental data for the spatial discharge structure and the current/voltage discharge characteristics.

1 Introduction

Various gas-filled diodes are widely used in modern electro-technical devices. The tip-to-plane electrodes system represents probably the most common design of a gas diode unit with strongly non-uniform configuration of an electric field. Namely they are used as spark-gap high-voltage switches [1] as well as the main component of technological devices for the discharge plasma surface treatment [2]. Therefore, major theoretical problems of the discharge development in such a system are intensively investigated by using of various theoretical simulation approaches [2]-[4].

The discharges in the gas-filled diodes are attractive due to the non-trivial switching characteristics and the low-temperature plasma parameters. Among the switching parameters, the breakdown formation time and the corresponding voltage amplitude are the most important. Plasma parameters, e.g. its spatial structure or its plasma-chemical composition are also of great importance, especially w.r.t. time-dependent studies. While the switching characteristics can be easily measured experimentally, the measurements of plasma parameters is much more complicated. That is the main reason to perform a theoretical simulation of gas discharge.

At present, we have a rather extensive base of experimental studies of this type of discharge, including performed with a picosecond and subnanosecond time resolutions, as well as with time synchronization of the measured signals. As part of the series of experimental studies done by groups of Russian and Chinese researchers [5], [6], a comparison can be made with the results of actual theoretical studies.

In this paper we use a two-moment "liquid" discharge plasma model [7] implemented in Plasma module of COMSOL Multiphysics 5.2 software. It allows modeling the time-dependent discharge propagation from the metal non-uniform electrode (tip) towards the second electrode (plane) accounting for all necessary plasma-chemical reactions. The main aim here is to simulate nanosecond gas discharge and accurately obtain the spatial discharge structure evolution.

2 Experimental Setup

The experimental setup is represented in **Fig. 1**. The triggering pulse from 1 provides a signal that the voltage pulse generator 2 transforms into a negative polarity voltage pulse with the amplitude values in the range of $U_0 \approx$ 27-30 kV with the rise time $t_f \approx$ 200 ns. The cathode here is a thin needle with diameter of 0.4 mm having the tip curvature radius of 0.1 mm, while the anode is a simple plane electrode. The distance between electrodes is equal to d = 9 mm. The nitrogen at 1 atm pressure with small (~2 %) oxygen admixture is used as the operating gas.

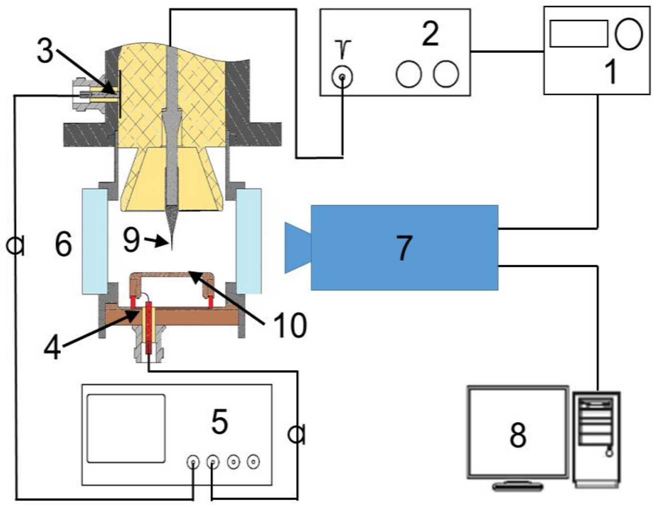

Fig. 1. The experimental setup: 1 – triggering pulse generator, 2 – pulsed voltage source, 3 – capacitive voltage divider, 4 – current shunt resistor, 5 – storage oscilloscope, 6 – output window, 7 – ICCD camera, 8 – personal computer, 9 – metal tip cathode, 10 - plane anode electrode.

Using the ICCD camera the sequence of instant images of the discharge dynamics was obtained (depicted at **Fig. 2**). Images from an ICCD camera are an integral picture of the glow of a non-stationary discharge, which, to a certain extent, can be compared with the distribution of the discharge plasma at a given point in time. Based on this comparison of experimental and theoretical data in the present work.

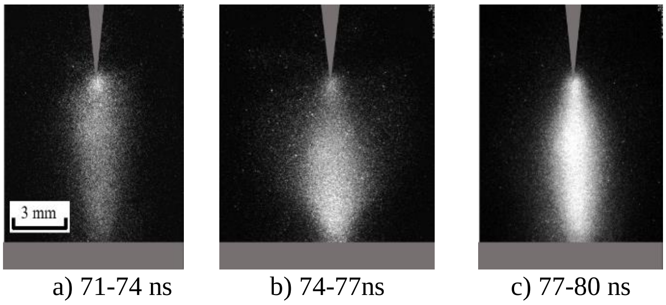

Fig. 2. Instant photographs from the ICCD-camera (gray areas depict electrodes).

3 Theoretical model

For the simplicity reasons a real three-dimensional diode in the model is substituted by the two-dimensional axisymmetric structure (**Fig. 3**).

The gas discharge model is based on the two-moment "liquid" model where charged particles movement is covered by the drift-diffusion approximation [7]. Since the discharge characteristic time is short, so the model implements only three important plasma-chemical reactions: the electron impact ionization $e + N_2 \rightarrow 2e + N_2^+$, molecular nitrogen dissociation $e + N_2 \rightarrow e + 2N$ and the photoionization $h\nu + N_2 \rightarrow e + N_2^+$.

The photoionization model we implement is based on the assumption 8 that the major contribution to the photoionization rate produces the radiation in the spectral range 980-1025 Å, where the radiation absorption by nitrogen N_2 can be omitted. The wavelength of 1025 Å is the natural threshold for the molecular oxygen photoionization reaction. Below the 980 Å, the radiation is strongly absorbed by nitrogen providing insignificant contribution to the production of photoelectrons. Taking into account the fine structure of the oxygen absorption spectrum, in the integral over the wavelength range 980-1025 Å in the general expression for the rate of photoionization was calculated and adopted for further computations.

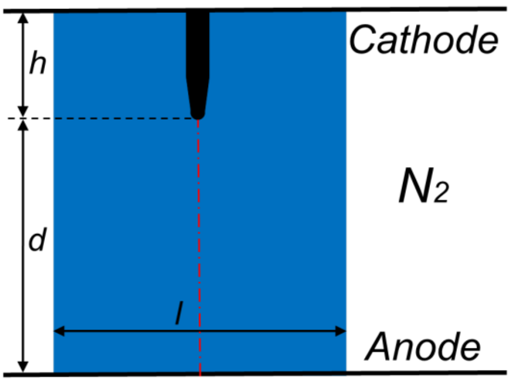

Fig. 3. The computational domain configuration (h = 1.6 mm, l = 4 mm, d = 9 mm).

We also note about the importance of taking into the account molecular nitrogen dissociation reaction as the main factor leading to electron energy losses [9]. Other plasma-chemical reactions typical to nitrogen e.g. involving ions of atomic nitrogen are omitted due to their smaller contribution to the fast discharge development. For the same reasons we also exclude different kinds of neutral excited species.

Electron component are described by the following equations system:

$$\begin{cases} \dfrac{\partial n_e}{\partial t} + \nabla \cdot \boldsymbol{\Gamma_e} = R_e \\ \dfrac{\partial n_\varepsilon}{\partial t} + \nabla \cdot \boldsymbol{\Gamma}_\varepsilon + \boldsymbol{E} \cdot \boldsymbol{\Gamma_e} = R_\varepsilon \end{cases} \quad (1)$$

where n_e is the electron number density, n_ε is the electron energy density, t is the time variable, $\boldsymbol{E}$ is the electric field strength. The source coefficients R_e and R_ε are defined by

$$\begin{aligned} R_e &= k_{ion}\left(\bar{\varepsilon}\right) n_n n_e + S_{ph}, \\ R_\varepsilon &= k_{ion}\left(\bar{\varepsilon}\right) n_n n_e + k_{diss}\left(\bar{\varepsilon}\right) n_n n_e, \end{aligned} \quad (2)$$

where $k_{ion}(\bar{\varepsilon})$ is the ionization rate as a function on mean electron energy, $\bar{\varepsilon} = n_\varepsilon / n_e$, n_n is the total neutral number density, $k_{diss}(\bar{\varepsilon})$ is the dissociation rate coefficient, S_{ph} is the photoionization rate.

Ion component describes by

$$\frac{\partial n_i}{\partial t} + \nabla \cdot \boldsymbol{\Gamma_i} = R_e, \quad (3)$$

where n_i is the N_2^+ number density.

The electron, electron energy and ion density fluxes $\boldsymbol{\Gamma_e}$, $\boldsymbol{\Gamma}_\varepsilon$ and $\boldsymbol{\Gamma_i}$ respectively, are given by the expressions

$$\begin{aligned} \boldsymbol{\Gamma_e} &= -n_e \mu_e \boldsymbol{E} - D_e \nabla n_e \\ \boldsymbol{\Gamma}_\varepsilon &= -\frac{5}{3} n_\varepsilon \mu_e \boldsymbol{E} - \frac{5}{3} D_e \nabla n_\varepsilon, \\ \boldsymbol{\Gamma_i} &= -n_i \mu_i \boldsymbol{E} - D_i \nabla n_i \end{aligned} \quad (4)$$

where μ_e and μ_i are the electron and ion mobilities, D_e and D_i are the electron and ion diffusivities.

The electric field is accounted self-consistently in the model by implementing the Poisson's equation:

$$\varepsilon_0 \nabla \cdot \boldsymbol{E} = -q\left(n_i - n_e\right), \quad (5)$$

where, q is the elementary charge, ε_0 is electrical constant.

The photoionization rate S_{ph} is implemented in the "differential" formulation i.e. based on the numerical solution of Helmholtz equations set

$$\nabla^2 S_{ph} - \Lambda_{ph}^{-2} S_{ph} = -G_{ph} R_e, \tag{6}$$

as described in [10]. Here, Λ_{ph} is effective photon path length, G_{ph} is coefficient of conversion of ionization rate R_e into photon radiation.

We use uniform plasma number density not exceeding 10^3 cm^{-3} and zero electric field and photoionization rate S_{ph} as the initial conditions. Boundary conditions are given in terms of generalized expressions for the particle and the electron energy density fluxes on solid electrode walls [11]

$$\begin{gathered}
\boldsymbol{\Gamma_e} \cdot \boldsymbol{n} = \frac{1}{4} n_e \bar{v}_e - \gamma\left(\boldsymbol{\Gamma_i} \cdot \boldsymbol{n}\right) + \mu_e n_e \left(\boldsymbol{E} \cdot \boldsymbol{n}\right), \\
\boldsymbol{\Gamma_i} \cdot \boldsymbol{n} = \frac{1}{4} n_i \bar{v}_i + \mu_i n_i \left(\boldsymbol{E} \cdot \boldsymbol{n}\right), \\
\boldsymbol{\Gamma_\varepsilon} \cdot \boldsymbol{n} = \frac{1}{2} n_\varepsilon \bar{v}_e - \bar{\varepsilon} \cdot \gamma\left(\boldsymbol{\Gamma_i} \cdot \boldsymbol{n}\right),
\end{gathered} \tag{7}$$

where $\boldsymbol{n}$ is the normal vector to the wall surface, $\bar{v}_e$ and $\bar{v}_i$ are the electron and ion thermal velocities, respectively, $\gamma = 0.1$ is the secondary electron emission coefficient of ion-wall interaction in nitrogen.

The simulation also accounts the contribution of field emission (autoelectronic emission) from the cathode surface due to the increase of an electrostatic field near the emission centers formed by metallic surface roughness. This electron flux is given in terms of Fowler-Nordheim expression from paper [12].

The complete discharge plasma system of equations (1)−(4) is solved in COMSOL Multiphysics software with Plasma Module implementing above two-moment model DC-discharge physics. Prior to this, the ionization rates and electron mobility were calculated using the BOLSIG+ solver [13] except the dissociation rate coefficient that was taken from [9].

We compare the simulation results according to two discharge models. In the first one (I) the photoionization was not included, while the second model (II) implements all enlisted elementary processes. The following simulation results of calculations are the refinement of preliminary computations of a similar discharge type presented in the conference paper [14].

4 Simulation results

The comparison of voltage time-profiles is shown in **Fig. 4** (switching characteristics) for both discharge models. We assume the breakdown formation to be a time-point having the maximum voltage at the discharge gap. The breakdown occurs at $t_{breakdown} \approx 92$ ns ($U_{breakdown} \approx 12$ kV) for both simulation regimes (with photoionization and without it). The presence of photoionization just slightly reduces the breakdown voltage value by no more than 50 V. Such difference is negligibly small, so we can assume that the switching characteristics of two modes are practically identical.

The discharge evolution is demonstrated in the sequence of static images at **Fig. 5**. In both cases the discharge initiation occurs approximately at the time point of t = 50 ns. The movement of the plasma channel begins with the expansion of the initial cathode formation in both spatial directions. After that, approximately from the time point of t = 80 ns, the formation of a plasma tip on the spherical plasma cloud surface occurs. This tip is the main channel of the discharge, which slightly expands in the radial direction during the motion. The formation of the initial spherical distribution is associated with the intense losses of the electron energy in the electron impact N_2 dissociation reaction. After the electric field exceeds the Lozansky-Firsov criterion threshold value, the rapid ionization wave development from the spherical layer surface starts. The process ends with the discharge gap switching stage at the time point of the gap intersection with the ionization wave channel (t = 90 ns). The gap voltage drop and the corresponding significant increase of the total discharge current accompany this.

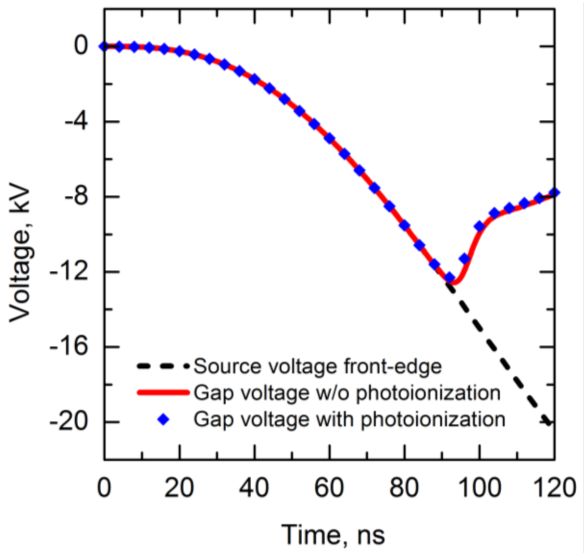

Fig. 4. Discharge voltage time-profiles.

Comparison of calculations with photoionization and without it shows that the effect of the latter on the development of a gas discharge is insignificant if the electron impact dissociation reaction of molecular nitrogen is included in the model. Also, the quantitative characteristics of the plasma do not change. The significant increase of the oxygen partial pressure in photoionization model, and hence the fraction of oxygen in gas mixture will probably lead to a visible change in the spatial discharge structure, but also the simulation will require more accurate plasma-chemical reaction set. Nevertheless, one this paper aims is to investigate the influence of minor electro-negative mixture to the discharge formation and evolution.

Additionally the parameters of runaway electrons have been calculated in order to discover their influence on the discharge dynamics. The calculations were based on the "hybrid" theoretical approach, involving principles of physical kinetics described in [15]. The results show, that the runaway electron current passing through the anode is too small compared to the full discharge current, so the influence of the runaway electrons on the discharge is negligible. Such conclusions are connected with the long rise time (more than 100 ns) of the operating voltage pulse.

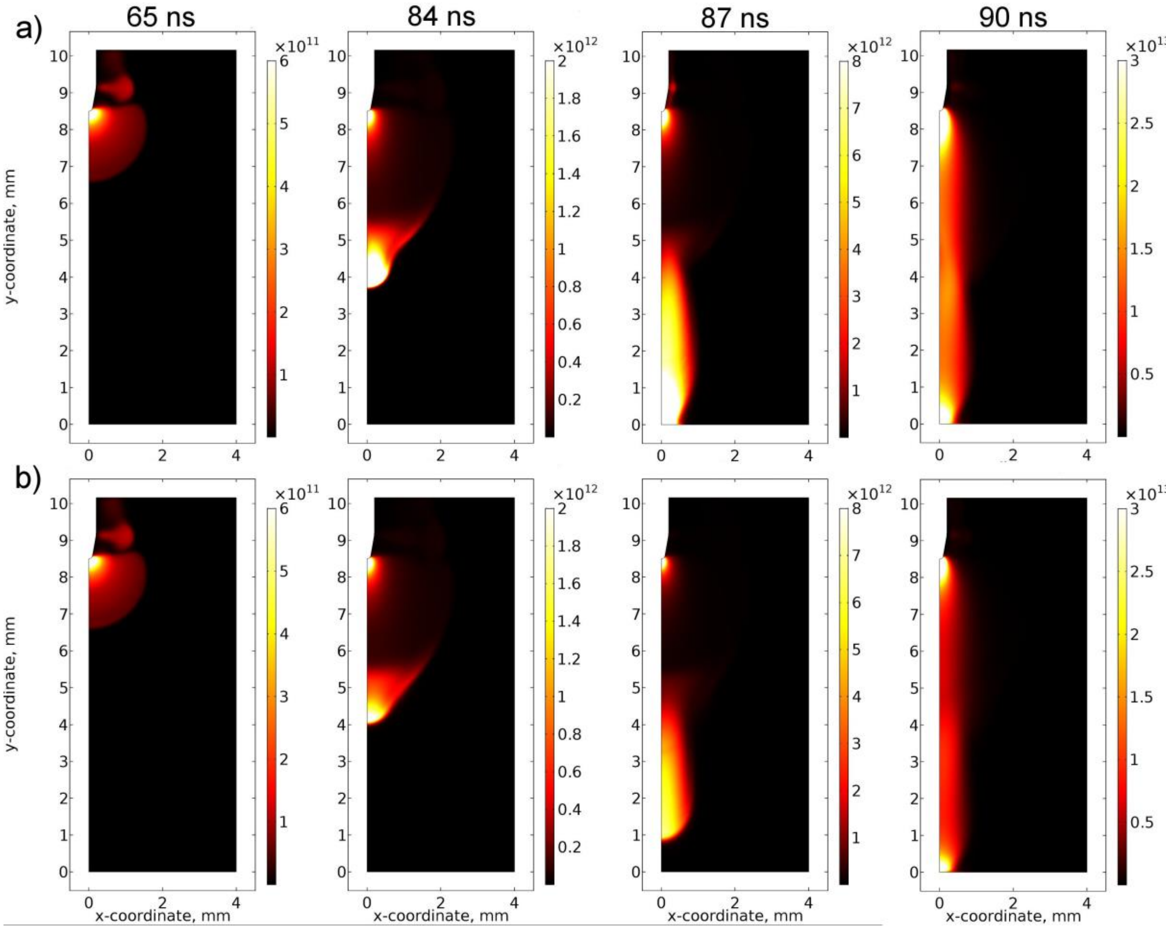

Fig. 5. Spatial distribution of the electron number density (scale in cm^{-3}) for gas discharge a) without and b) with photo-ionization process for the same time points.

5 Conclusions

The simulation of the gas-filled diode breakdown in the tip-to-plane electrodes configuration shows good agreement with the existing experimental data. Current theoretical study shows that the gas photoionization is insignificantly affects the discharge spatial structure for the positive polarity of the anode voltage. It was also shown that in gas mixtures containing valuable amount of nitrogen the electron impact dissociation plays an important role in the formation of spatially-inhomogeneous discharge structure.

References

1. G. Schaefer, M. Kristiansen, and A. Guenther, Eds., "Gas Discharge Closing Switches," Springer-Verlag US, 1990.
2. Y. Akishev, O. Goossens, T. Callebaut, C. Leys, A. Napartovich, and N. Trushkin, "The influence of electrode geometry and gas flow on corona-to-glow and glow-to-spark threshold currents in air," Journal of Physics D: Applied Physics, vol. 34, no. 18, pp. 2875–2882, 2001.
3. S. Iseni, S. Dozias, J.-M. Pouvesle, and E. Robert, "Experimental study of ultra-fast electric field in an atmospheric pressure discharge in a pin-to-plate geometry," 2016 IEEE International Conference on Plasma Science (ICOPS), 2016.
4. O. Eichwald, M. Yousfi, O. Ducasse, N. Merbahi, J. P. Sarrette, M. Meziane, and M. Benhenni, "Electro-Hydrodynamics of Micro-Discharges in Gases at Atmospheric Pressure," Hydrodynamics - Advanced Topics, 2011.
5. Tao Shao, Cheng Zhang, Zheng Niu, Ping Yan, V. F. Tarasenko, E. K. Baksht, A. G. Burahenko, and Y. V. Shut'ko, "Diffuse discharge, runaway electron, and x-ray in atmospheric pressure air in an inhomogeneous electrical field in repetitive pulsed modes," Applied Physics Letters, vol. 98, no. 2, p. 021503, 2011.
6. Tao Shao, V. F. Tarasenko, Cheng Zhang, E. K. Baksht, Dongdong Zhang, M. V. Erofeev, Chengyan Ren and Y. V. Shutko, "Diffuse discharge produced by repetitive nanosecond pulses in open air, nitrogen, and helium," Journal of Applied Physics, vol. 113, no. 9, p. 093301, 2013.
7. E. Gogolides and H. H. Sawin, "Continuum modeling of radio-frequency glow discharges. I. Theory and results for electropositive and electronegative gases," Journal of Applied Physics, vol. 72, no. 9, pp. 3971–3987, 1992.
8. A. A. Kulikovsky, "Two-dimensional simulation of the positive streamer in N2between parallel-plate electrodes," Journal of Physics D: Applied Physics, vol. 28, no. 12, pp. 2483–2493, 1995.
9. P. C. Cosby, "Electron-impact dissociation of nitrogen," The Journal of Chemical Physics, vol. 98, no. 12, pp. 9544–9553, 1993.
10. A. Bourdon, V. P. Pasko, N. Y. Liu, S. Célestin, P. Ségur, and E. Marode, "Efficient models for photoionization produced by non-thermal gas discharges in air based on radiative transfer and the Helmholtz equations," *Plasma Sources Science and Technology*, vol. 16, no. 3, pp. 656–678, 2007.
11. V. Y. Kozhevnikov, A. V. Kozyrev, A. V. Batrakov, N. S. Semeniuk, and V. M. Karaban, "Diagnostics of primary arcing in electronics of satellite telecommunication systems," *2015 23rd Telecommunications Forum Telfor (TELFOR)*, pp. 615-618, 2015.
12. A. V. Kozyrev, Y. D. Korolev, and G. A. Mesyats, "Autoemission processes and Transition from the glow-discharge to Arc-discharge," *Zhurnal Tekhnicheskoi Fiziki*, vol. 57, no. 1, pp. 58−64, 1987.

13. G. J. M. Hagelaar and L. C. Pitchford, "Solving the Boltzmann equation to obtain electron transport coefficients and rate coefficients for fluid models," *Plasma Sources Science and Technology*, vol. 14, no. 4, pp. 722–733, 2005.
14. V. Y. Kozhevnikov, A. V. Kozyrev, N. S. Semeniuk, and A. O. Kokovin, "Theoretical Simulation of Nanosecond High Pressure Gas Discharge in the Pin-to-Plate Gap," *2018 26rd Telecommunications Forum Telfor (TELFOR)*, pp. 442-445, 2018.
15. A. Kozyrev, V. Kozhevnikov, M. Lomaev, D. Sorokin, N. Semeniuk, and V. Tarasenko, "Theoretical simulation of the picosecond runaway-electron beam in coaxial diode filled with SF6 at atmospheric pressure," *EPL (Europhysics Letters)*, vol. 114, no. 4, p. 45001, 2016.